Bioresource Technology 200 (2016) 90–102

Contents lists available at ScienceDirect

Bioresource Technology

journal homepage: www.elsevier.com/locate/biortech

Modeling of biomass fractionation in a lab-scale biorefinery: Solubilization of hemicellulose and cellulose from holm oak wood using subcritical water

A. Cabeza [a], C.M. Piqueras [b], F. Sobrón [a], J. García-Serna [a,*]

[a] High Pressure Processes Group, Department of Chemical Engineering and Environmental Tech., University of Valladolid, 47011 Valladolid, Spain
[b] Planta Piloto de Ingeniería Química, PLAPIQUI-Universidad Nacional del Sur-CONICET, Camino La Carrindanga km 7, 8000 Bahía Blanca, Buenos Aires, Argentina

HIGHLIGHTS

- Hydrothermal fractionation of holm oak was studied in a packed bed reactor.
- Temperature has the main influence over the composition out flow stream.
- A kinetic model was developed which is able to reproduce the profile of TOC content.
- The model is capable to reproduce all the physical phenomena like porosity variation.
- A simulation of the whole process was done, checking its physical behavior.

GRAPHICAL ABSTRACT

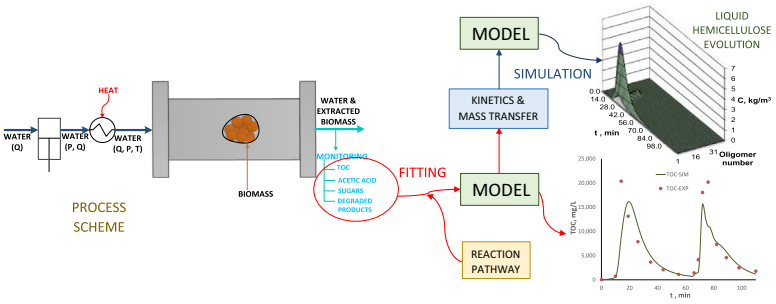

ARTICLE INFO

Article history:
Received 23 July 2015
Received in revised form 16 September 2015
Accepted 18 September 2015
Available online 26 September 2015

Keywords:
Holm oak
Hydrothermal fractionation
Subcritical water
Biorefinery
Modeling

ABSTRACT

Lignocellulose fractionation is a key biorefinery process that need to be understood. In this work, a comprehensive study on hydrothermal-fractionation of holm oak in a semi-continuous system was conducted. The aim was to develop a physicochemical model in order to reproduce the role of temperature and water flow over the products composition. The experiments involved two sets: at constant flow (6 mL/min) and two different ranges of temperature (140–180 and 240–280 °C) and at a constant temperature range (180–260 °C) and different flows: 11.0, 15.0 and 27.9 mL/min. From the results, temperature has main influence and flow effect was observed only if soluble compounds were produced. The kinetic model was validated against experimental data, reproducing the total organic carbon profile (e.g. deviation of 33%) and the physicochemical phenomena observed in the process. In the model, it was also considered the variations of molecular weight of each biopolymer, successfully reproducing the biomass cleaving.

© 2015 Elsevier Ltd. All rights reserved.

1. Introduction

The concept of biorefinery is based on the definition of a conventional petroleum refinery. Therefore, it is an installation which transforms a raw material (biomass) into energy (heat, electricity and biofuels) and several products (chemicals and biomaterials) by fractionation or conversion processes. One of the most studied ways to perform this conversion is biomass pyrolysis, where heat is used to transform it into charcoal, gases and biofuels (Ranzi et al., 2008; Tanoue et al., 2007; Tock et al., 2010). On the other hand, hydrothermal fractionation is another promising option because it is capable to recover the cellulosic fraction of biomass, which corresponds between 38.3 and 81.3 wt% of woody biomass

* Corresponding author. Tel.: +34 983184934.
E-mail address: jgserna@iq.uva.es (J. García-Serna).

http://dx.doi.org/10.1016/j.biortech.2015.09.063
0960-8524/© 2015 Elsevier Ltd. All rights reserved.

Nomenclature

C_t	total concentration in the solid, mg/L
ε and φ	porosity of the bed and the relation factor between it and C_t, dimensionless
C_{S_j}, C_{S_i}	concentration of the compound "j" or "i" in the solid phase, mg/L
r_j	reaction rate of the compound "j", mg/min · L
$k_j \cdot a$	mass transfer coefficient multiplied by the specific exchange area, min^{-1}
$C^*_{L_j}$	equilibrium concentration of the compound "j" in liquid phase, mg/L
$\bar{C}_{L_j}$	average concentration of the compound "j" along the reactor in liquid phase, mg/L
H_j	equilibrium constant between the solid and the liquid, dimensionless
C_{L_j}, C_{L_i}	concentration of the compound "j" or "i" in the liquid phase, mg/L
$\alpha_{i,j} or \alpha_{j,i}$	stoichiometric coefficient of the compound "j" for the reaction "i", mg
k_{d_j}	kinetic constant of the compound "j", $mg^{-1} \cdot min^{-1}$
F_{auto}	auto catalytic factor for the solid kinetics, dimensionless
$\beta_{i,j}$ or $\gamma_{i,j}$	acceleration factor for the compound "j" in the reaction "i", dimensionless
m_i, m_{i_o}	solid mass and its initial value of the compound "i", mg
r_{dea_j}	deacetylation reaction rate for compound "j", mg/min · L
r_{dead}	reaction rate of the direct deacetylation of HC_1, mg/min · L
k_{dead}	kinetic constant of r_{dead}, $mg^{-1} \cdot min^{-1}$
r_{deadi}	first reaction rate of the direct deacetylation of HC_2, mg/min · L
k_{deadi}	kinetic constant of r_{deadi}, $mg^{-1} \cdot min^{-1}$
r_{deadii}	second reaction rate of the direct deacetylation of HC_2, mg/min · L
k_{deadii}	kinetic constant of r_{deadii}, $mg^{-1} \cdot min^{-1}$
r_{cv}	C5 formation from HC_1 reaction rate, mg/min · L
k_{cv}	kinetic constant of r_{cv}, $mg^{-1} \cdot min^{-1}$
r_{lent}	C6 formation from HC_1 reaction rate, mg/min · L
k_{lent}	kinetic constant of r_{lent}, $mg^{-1} \cdot min^{-1}$
C_{H^+}	proton concentration in liquid phase, mg/min · L
n_1, n_2	reaction order for proton concentration in hydrolysis and sugar degradation, dimensionless
k_{L_j}	kinetic constant for compound "j" in liquid phase, $L^{n1} \cdot mg^{-1-n1} \cdot min^{-1}$
$r_{\deg}$	reaction rate for sugar degradation, mg/min · L
$k_{\deg 1}$, k_{deg2}	kinetic constant for C6 and C5 degradation, $L^{n2} \cdot mg^{-1-n2} \cdot min^{-1}$
$C_{L_{i_{Sugar-C6}}}, C_{L_{i_{Sugar-C5}}}$	concentration of the sugar "C6" or "C5" number "i", mg/L
r_{de}	reaction rate for sugar deacetylation, mg/min · L
k_{de}	kinetic constant of r_{de}, $mg^{-1} \cdot min^{-1}$
$C_{L_{sugar}}$	total sugar concentration in liquid phase, mg/L
r_{rep}	reaction rate for the polymerization, mg/min · L
k_{rep}	kinetic constant of r_{rep}, $mg^{-1} \cdot min^{-1}$
r_{acet}	reaction rate for the acetic acid dissociation, mg/min · L
k_{direct}	kinetic constant of acetic acid dissolution, $mg^{-1} \cdot min^{-1}$
$k_{inverse}$	kinetic constant of acetic acid recombination, $L \cdot mg^{-2} \cdot min^{-1}$
$C_{L_{acet^-}}$	concentration of the acetate, mg/L
r_{prot}	proton consumption reaction rate, mg/min · L
k_{prot}	kinetic constant of r_{prot}, $mg^{-1} \cdot min^{-1}$
$A(T)$ or A	Napierian logarithm of the kinetic prexponential factor, dimensionless
$H_o(T)$	solubility constant, $°C^{-1}$
E_1, E_2	base activation energy and correction factor of the base activation energy depending on the molecular weight, J/mol
PD_j	polymerization degree of compound "j", dimensionless
PD_h	first correction factor of the PD_j for solubility calculations, dimensionless
h_p	second correction factor of the PD_j for solubility calculations, dimensionless
u	liquid velocity in the reactor, m/min
N	number of compounds, dimensionless
L	length of the reactor, m
z	dimensionless length of the reactor, dimensionless
t	operating time, min
X_{exp}, X_{sim}	experimental and simulated value of the fitted variable
n	total number of experiments, dimensionless

(Bobleter, 1994; Yedro et al., 2015), using only water as reactive. This technique has been highly studied and various articles can be found in literature (Charles et al., 2004; Mohan et al., 2015; Pronyk and Mazza, 2010; Rogalinski et al., 2008). However, the modelling of this process is an issue which still has not a final solution due to biomass complexity, which is formed by three main compounds: hemicellulose, cellulose and lignin. Cellulose and hemicellulose are polysaccharides composed by up to 10,000 and 200 monomers, respectively. The former is a linear biopolymer with a high degree of crystallinity formed by hexoses (C6) and the latter is amorphous and it is constituted by hexoses and pentoses (C5). On the other hand, lignin is an aromatic biopolymer formed by phenylpropane units (Bobleter, 1994; Harmsen et al., 2010). In addition, biomass diversity and the process monitoring also complicate the development and validation of a kinetic model. The first issue can be seen in Yedro et al., 2015 who studied the fractionation of several wood species in a semi-continuous reactor. They observed that the extraction yields were very different between the species, although the qualitative behavior of all of them were similar. Regarding monitoring, the problem would be that the analysis of the samples must be done at different conditions from which were used during the operation. The reason is that the characterization requires wet chemical analysis followed by a separation of the different fractions by conventional analytical instruments at certain conditions (Carrier et al., 2011). Therefore, some measured values would be different from the real ones during the operation.

To sum up, it is not clear that a model with a single set of kinetic parameters could be used as a global solution for biomass solubilization. Nevertheless, several models for this process, with a reasonable success, can be found in literature (Haghighat Khajavi et al., 2005; Lin et al., 2015; Mohan et al., 2015; Rogalinski et al., 2008; Zhu et al., 2014). Zhu et al. (2014) studied the hydrolysis of peanut shell in subcritical water in a batch reactor. They proposed a kinetic model with a 1st reaction order respect to biomass concentration which was able to reproduce their experimental data. In the same way, Mohan et al. (2015) and Lin et al. (2015) assessed the hydrolysis of real biomass (bamboo and rice straw respectively) in a batch reactor and they also fitted their data applying a 1st order kinetic. Rogalinski et al. (2008) performed a successful kinetic analysis of the starch hydrolysis in a plug-flow reactor assuming a 1st reaction order. And Haghighat Khajavi et al. (2005) studied the hydrolysis of sucrose in a flow-type reactor but taking into account the effect

of the pH variations during the process. All of them were based on the idea that the cellulosic fractions of biomass (cellulose and hemicellulose) decompose into sugar. This sugar formation could be from an intermediate product (oligomers) or directly from biomass. The formation of degradation products, such as formic or lactic acid, from these sugars was also considered. Nonetheless, they were generally applied to a batch system or they studied model compounds, like sucrose. Besides, they did not take into account the whole set of physical phenomena observed during a hydrothermal treatment of biomass: deacetyla tion/autohydrolysis/pH variations and solid–liquid mass transfer/porosity variations. In addition, a previous work (Cabeza et al., 2015) was done to reproduce the behavior of a hemicellulose extraction process from holm oak (one of the most common trees in southern Spain) considering all these phenomena. The study was performed in a packed bed reactor with hot compressed water and the effect of different particle diameters and flow rates was also assessed. Temperature was fixed around 180 °C in order to enhance hemicellulose extraction. The result was a model able to reproduce the total organic carbon (TOC), pH and acetic acid concentration at the reactor output with average absolute deviations of 32.1%, 7.4% and 56.0% respectively. However, the effect of the molecular weight, the oligomer distribution and high temperature effect were not considered with this model.

Therefore, the objective of this work is to complete that preliminary kinetic model for the holm oak hydrothermal fractionation in a semi-continuous system (packed bed reactor) with hot compressed water. This model will be able to reproduce the experimental data including the effect of the molecular weight and all the physical phenomena observed. Besides, it will also capable of simulating the oligomer distribution and reproducing the variations in the fractionation when high and low temperatures are used. The latter was done performing a temperature change during the process. So, the extraction of the whole cellulosic of biomass at subcritical conditions has been studied. The idea was to perform experiments at two temperatures, one between 140 and 180 °C, in order to enhance hemicellulose extraction, and the other between 240 and 280 °C to recover the main cellulose fraction. An autocatalytic kinetic was used being suitable to reproduce the fractionation in the previously mentioned study. Thus, this model will help to understand better the fractionation process. In addition, it will allow to simulate how a change in the reactor diameter or length would affect the fractionation and how would be the solid composition evolution, which could be an important factor to stop the process. To sum up, this model will be a useful tool to perform a future scale-up of this lab-scale biorefinery.

2. Methods

2.1. Experimental setup

The experimental device used in this work is shown in Fig. 1. The whole system consisted in a fractionation column whose output stream feeds a supercritical hydrolysis reactor. This setup belongs to a bigger project and it was constructed with the aim to study other biomass transformations (e.g. enhancement of sugars yield and optimizing the selectivity to fully hydrolyzed products, coming from cellulose or from real biomass). However, for this work only the fractionation column was used. The system was composed of a water deposit (T-1) followed by an American Lewa EK6 2KN high pressure pump (P-1, maximum flow rate 1.5 kg/h) and a pre-heater (H-1, 200 cm of 1/8″ SS 316 pipe, electrically heated by 2 resistances of 300 W) used to maintain a constant temperature at the inlet of the fractionation column (R-1, a SS 316 tube of 40 cm length and 1.27 cm O.D.). In addition, the column was heated by three flat resistors of 500 W placed along an aluminum device which contains the column. The preheater and the column were inside a chromatographic oven HP5680 for safety reasons.

On the other hand, the supercritical water line was composed by another tank of water (T-2), a heater (H-2, a SS316 tube of 20 m with 1/8 in O.D.) with two flat resistors, total power of 5 kW and a Milton Roy XT membrane pump (P-2, maximum flow rate 6 kg/h). Pressure was controlled by a Micro Metering valve 30VRMM4812 from Autoclave Engineers (V-4). The output of the reactor (R-2) was cold down in the heat exchanger H-3 (200 cm of concentric tube 1/2–1/4 in.) with cold water and then it was collected in the tank T-4.

2.2. Procedure

6.12 ± 0.03 g of holm oak were introduced into the fractionation column. Two metallic filters were used, one located at the top and the other at the bottom, to keep the raw material inside. In order to check if any leak was present in the fractionation line, cold water was pressurized into the system before each experiment. Then, the flow was stopped and the preheater and the fractionation column were heated up. When the desired temperature value was achieved the pumps were turned on adjusting the flow in the pump control panel and the pressure with V-4. In order to monitoring the process, pH evolution was followed online (every minute) using an electronic pH-meter (Nahita model 903). Also, liquid samples were taken between 2 and 20 min (in tank T-3), depending on the pH value. During the operation, two temperatures were used. The change between them was done depending

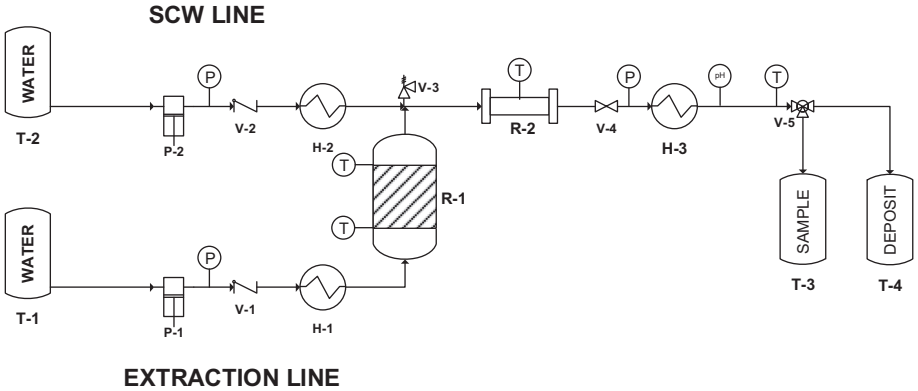

Fig. 1. Process flow diagram of the experimental device. T-1 and T-2: type II Millipore water tanks, P-1: high pressure piston pump. P-2: membrane pump, V-1 and V-2: Parker check valve. H-1: electric low temperature heater. H-2: high temperature heater. R-1: fractionation column. V-3: Parker relieve valve. R-2: supercritical reactor. V-4: high temperature valve, HE: cooling heat exchanger. V-5: three way Parker valve, T-3: Falcon flask. T-4: product vessel.

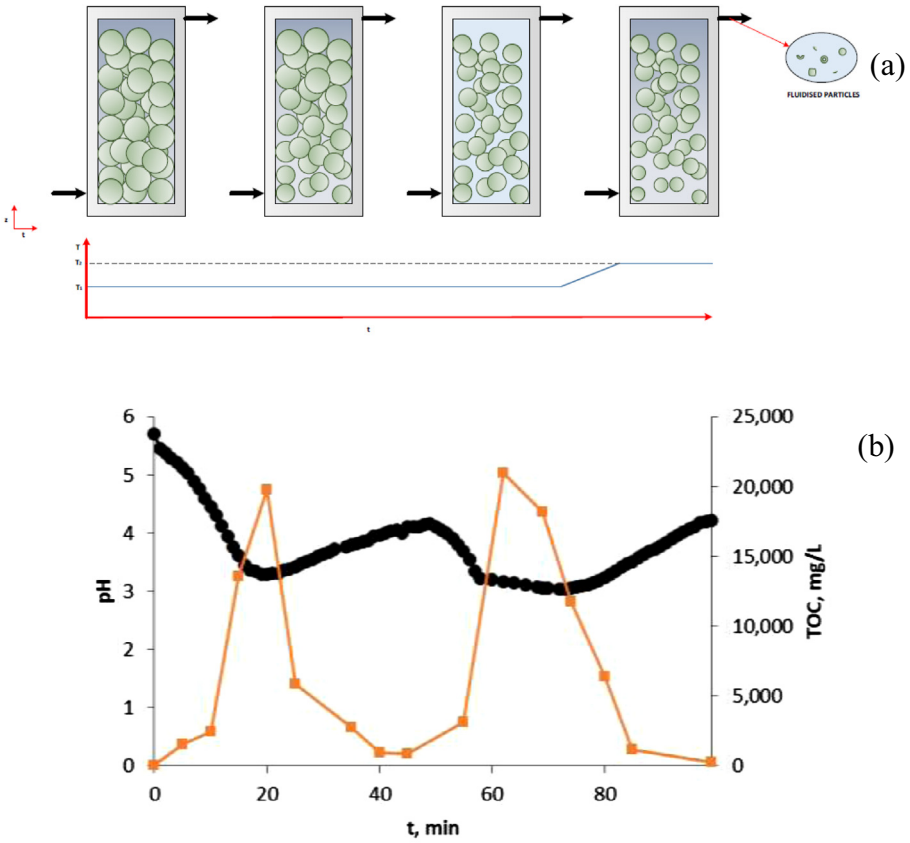

Fig. 2. Scheme of the hydrothermal degradation of biomass at two temperatures (a) and pH evolution during the process (b).

on the value of the monitored pH, because of the fact that there is a relation between the pH value and the extracted biomass. So, if the pH variation is slow, biomass has reached its maximum solubilization at that temperature and the temperature change is done (Fig. 2b).

Once the operation was over, the heating was shut off and the fractionation column was gradually cooled down to room temperature with external air flux. Both pumps were disconnected and the system was depressurized. The solid inside of the reactor was collected, filtered and dried 24 h at 105 °C for further analysis. Finally, the column was cleaned and reconnected to the system, which was washed with Type II water.

2.2.1. Effect of the temperature

In previous studies it has been seen that temperature is the main influencing variable on this type of process. For this reason, 8 different temperatures (140, 150, 160, 180, 240, 250, 260 and 280 °C) were studied in this work. Besides, the same sample was treated at two different temperature levels in order to extract first the hemicellulose at the lowest temperature and then the cellulose at the highest temperature. The volumetric flow was fixed around 6 mL/min and the operating pressure was 15 MPa.

2.2.2. Effect of the volumetric flow

Other variable that have a high effect in the biomass solubilization is the volumetric flow. This was studied by performing experiments at 3 different flows (11.0, 15.0 and 27.9 mL/min) at the same temperatures (180–260 °C).

2.2.3. Model validation

In order to validate the model, TOC, sugars, acetic acid and degradation product concentration at the output of the column were measured and fitted. The adjustment was focused in TOC because it would be the most precise measure. This would be caused by the high dilution (Table 1) of the samples due to the fact that during the operation both pumps must be working (Fig. 1). Besides, the final mass inside the reactor was simulated and compared with the experimental data. In addition, the overall behavior of the system was simulated. To achieve these objectives the experiments arrayed in Table 1 were performed.

Table 1
Experiments performed and its operational conditions.

Experiment	Volumetric flow mL/min	Sampling volumetric flow mL/min	Range of temperatures °C	Operating time min
1	6.5	22.8	180–280	99
2	6.2	22.5	160–260	120
3	7.8	23.4	150–250	160
4	6.9	21.1	140–240	200
5	6.5	23.1	180–260	110
6	11.5	37.7	180–260	110
7	15.0	100.8	180–260	60
8	27.0	106.8	180–260	46

2.3. Analytical methods

2.3.1. Solid characterization

The solid phase characterization was done following the method provided by the National Renewable Energy Laboratory (NREL) – Determination of Structural Carbohydrates and Lignin in Biomass. Firstly, biomass suffered an extraction performed in a Soxhlet equipment by n-hexane. After, a sample of 300 mg (m) was treated with 3 mL of sulphuric acid (72 wt%) for 30 min at 30 °C. Then, the sample was diluted by 84 mL of distilled water

and it was maintained at 120 °C for one hour more. The result was filtered under vacuum, washed by distilled water and dried at 105 °C for 24 h. Then, the solid was weighted (m_1) and calcined at 550 °C for 24 h and weighted (m_2) again. Thus, the acid insoluble lignin was obtained by $(m_1 - m_2)/m$. The obtained liquid was used to determine the content of acid soluble lignin by spectrophotometry, measuring the absorbance at 320 nm (recommended absorptivity $34\ L \cdot g^{-1} \cdot cm^{-1}$). Moreover, 30 mL of sample were neutralized up to pH = 6–7 with calcium carbonate and they were filtered by 0.2 μm filters. Finally, this sample was analyzed by high pressure liquid chromatography (HPLC). The used HPLC column was SUGAR SH-1011 (Shodex). As mobile phase a 0.01 N sulfuric acid solution and Milli-Q water were used. To obtain the hemicellulose, cellulose and degradation product content two detector were used: a Waters IR detector 2414 (210 nm) and Waters dual λ absorbance detector 2487 (254 nm). The calculated initial composition of the biomass sample is: 1.81 wt% of extractives with n-hexane, 46.64 wt% of cellulose, 24.48 wt% of hemicellulose, 27.07 wt% of lignin and 0.28 wt% of ash. The value of the lignin includes the soluble lignin (4.32%).

2.3.2. Liquid characterization

An acid hydrolysis was performed to the liquid phase in order to convert the oligomers into their monomeric sugars. Samples of 10 mL were hydrolyzed by 4 mL of sulphuric acid (72 wt%) and maintaining them for 30 min at 30 °C. After, the sample was diluted by 86 mL of distilled water and it was incubated for one hour more at 120 °C. Then, it was neutralized with calcium carbonate until pH = 6–7 and filtered using 0.2 μm filters. Finally, it was analyzed by HPLC as explained in the before section. In addition, the total organic carbon (TOC) was measured by Shimadzu equipment model TOC-VCSH. The carbon concentration of the standard solutions corresponds to 500 mg C/L.

3. Comprehensive modeling

3.1. Fractionation process by hydrothermal processes at mild temperatures

The fractionation takes place in solid phase where hemicellulose and cellulose start to break into oligomers of decreasing molecular weight. For both species, at a certain molecular weight, they became water-soluble and they are solubilized. From this point, the fractionation occurs as in solid phase as in liquid phase. In the latter, the solubilized oligomers hydrolyze, cleaving down in smaller oligomers until they reach their respective monomers (sugars). Finally, these monomers, depending on temperature and residence time, can be transformed into several degradation products, such as hydroxymethylfurfural, formic acid, lactic acid and others (Alvarez-Vasco and Zhang, 2013; Feng et al., 2012; Yedro et al., 2015). Basically, the reactor behaves like a fixed bed extraction-reaction column (Fig. 2a). Therefore, solid is depleted from bottom to top and liquid is more concentrated at the outlet. This process continues up to all the removable biomass at the operating is recovered. Reached this point, a change in the operating temperature is performed, and the extraction process starts again. This new extraction could originate a thermal breaking process in the biomass sample, which means that some parts of the solid might be separated from the whole biomass and they might be fluidized outside of the fractionation column.

3.2. Reaction pathway

The proposed reaction mechanism is shown in Fig. 3a. As it was mentioned in Section 1, the aim was to reproduce the experimental behavior of the reactor taking into account the main phenomena of the process, i.e. biomass cleaving and solubilization, biomass hydrolysis, changes in porosity and pH variations. To this end, for both, cellulose and hemicellulose, a population of several oligomers of decreasing length was used. In addition, deacetylation reactions were considered for hemicellulose family (Garrote et al., 2002; Parajó et al., 2004). Besides, a proton consumption reaction was introduced because it was observed some pH increments at the start of the operation. So, it was assumed that a certain amount of inorganic compounds with basic behavior was present in biomass. This value was initially fixed at 1% in order to provide enough substance to the neutralization but without disturbing the initial composition. On the other hand, two kinds of hemicellulose and cellulose were defined, one easily degradable and other hard to break (Charles et al., 2004; Klemm et al., 2005). For the former, this could be caused by a structural reason, the fact that some hemicellulose fibers can be protected by cellulose and lignin, which reduces their breaking. Regarding cellulose, the reason would be that there is a certain fraction of cellulose which could not be crystalline. This subdivision means that each type of cellulose and hemicellulose has its own oligomer population (OP). The OP for both hemicelluloses was formed by 60 compounds each, 40 for the fibers which were not deacetylated and 20 for the fibers deacetylated. For cellulose, both populations also had 60 members. These OP were used to reproduce in a more real way the biomass cleaving into smaller and smaller species (Fig. 3b). In addition, it was assumed that cellulose fibers have 10,000 units and hemicellulose fibers 200 (Charles et al., 2004). In both cases, compounds from 1 to 20 units were simulated and the rest of the family was formed by oligomers with increments of 250 and 9 units respectively. So, for cellulose, its fiber would contain 10,000 units, the highest oligomer, 9770 units and the following oligomer 9520 units. For hemicellulose, its fiber would be formed by 200 units, the highest oligomer by 191 and the following by 182. In parallel, direct deacetylation reaction from both hemicelluloses, direct dimer and monomer (sugars C6) formation and direct oligomer and monomer (sugars C5) formation from hemicellulose easily degradable were also included. These two last reactions, were needed to reproduce the initial slow solubilization of biomass. Finally, hexoses (C6) formation from hemicellulose (Charles et al., 2004), sugar degradation, and polymerization reactions from degradation products (Kumar et al., 2010; Minowa et al., 1998) were considered too.

3.3. Kinetic model

In order to simplify the problem the following statements were assumed: (1) there are nor temperature neither concentration profiles within the solid along the reactor length, (2) the solid porosity only depends on the total concentration of the solid phase, (3) there are not significant diffusional effects in the solid or liquid phase, (4) lignin behaves as an inert at these temperature conditions, taking as negligible soluble lignin and (5) the reaction order for all the kinetics is 1 for the biomass compound.

3.3.1. Mass balances

3.3.1.1. Solid phase. The model was obtained applying a mass balance for each compound (Eq. (1)). In order to introduce the effect of the porosity variations, the definition of the porosity (Eq. (2)) was introduced in Eq. (1), obtaining Eq. (3).

$$\frac{d(1-\varepsilon)\cdot C_{S_j}}{dt} = r_j - k_j \cdot a \cdot \left(C^*_{L_j} - \bar{C}_{Lj}\right) \tag{1}$$

$$\varepsilon = 1 - \varphi \cdot C_t \tag{2}$$

$$\frac{dC_{S_j}}{dt} = \frac{1}{1-\varepsilon}\cdot\left[r_j - \varphi \cdot C_{S_j}\cdot\frac{dC_t}{dt} - k_j \cdot a \cdot \left(C^*_{L_j} - \bar{C}_{L_j}\right)\right] \tag{3}$$

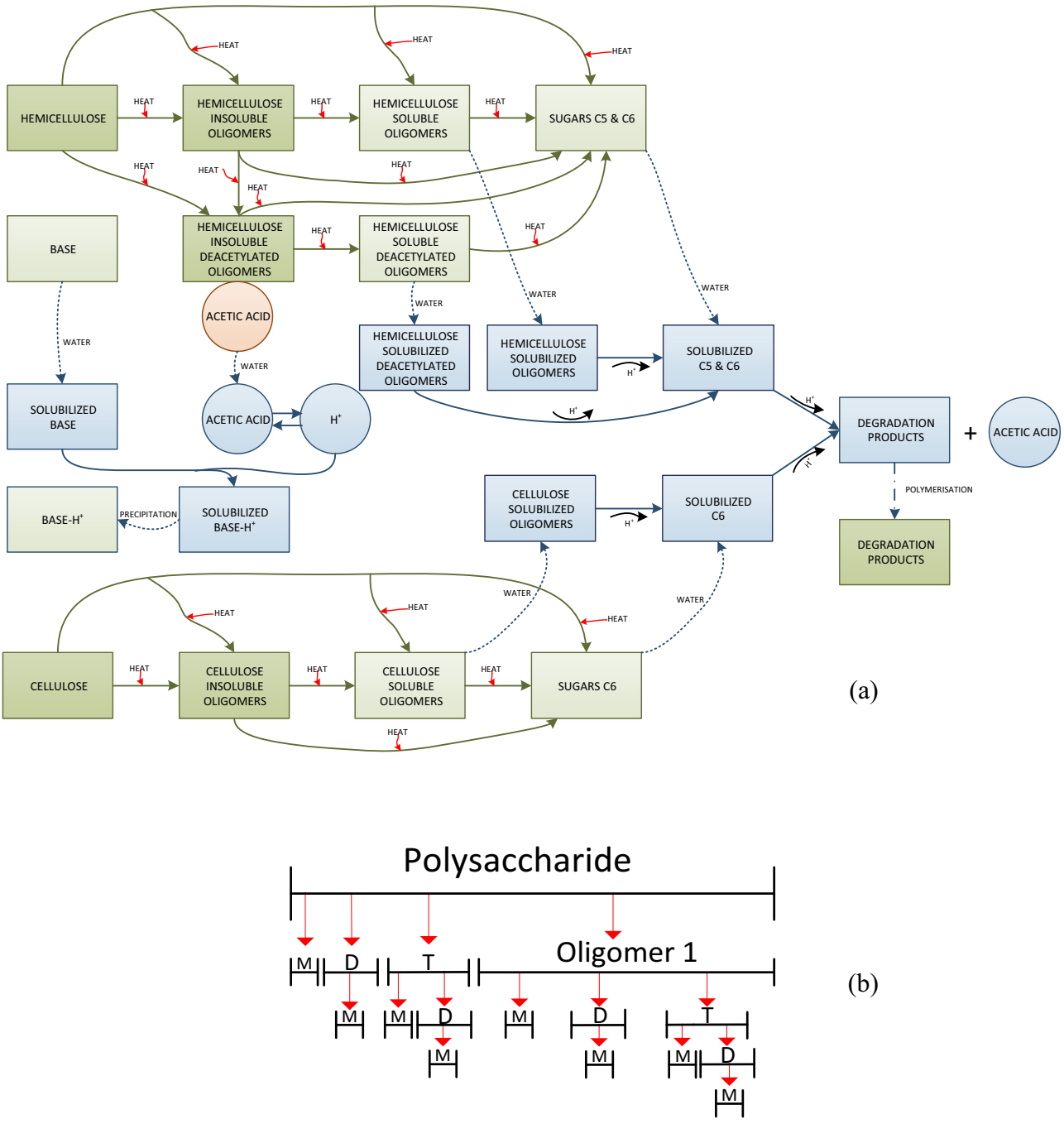

Fig. 3. Reaction pathway (a). Polysaccharide cleaving (b). M: monomer. D: dimer. T: trimer.

On the other hand, the mass balance to the insoluble lignin, considered as an inert compound, would be Eq. (4).

$$\frac{d(1-\varepsilon)\cdot\left(C_t-\sum_{j=1}^{j=N}C_{S_j}\right)}{dt}=0 \tag{4}$$

3.3.1.2. Liquid phase. Developing a similar process to the solid phase, the mass balance for each liquid compound would be represented by Eq. (5).

$$\frac{\delta C_{L_j}}{\delta t}=\frac{1}{\varepsilon}\cdot\left[r_j-\frac{u}{L}\cdot\frac{\delta C_{L_j}}{\delta z}-\varphi\cdot C_{L_j}\cdot\frac{dC_t}{dt}+k_j\cdot a\cdot\left(C^*_{L_j}-\bar{C}_{L_j}\right)\right] \tag{5}$$

3.3.2. Kinetics

3.3.2.1. Solid phase. Solid kinetics were based on an autocatalytic model (6) due to the fact that it has been successfully used by other authors (Capart et al., 2004) to reproduce the sudden changes in biomass at certain temperature. In addition, depending on the population this autocatalytic factor changes its definition. So, the auto catalytic factor (F_{auto}) for the hemicellulose (HC_1) and cellulose (C_1) easily degradable is shown in Eq. (7). And for the hard hemicellulose (HC_2) and cellulose (C_2) is shown in Eq. (8).

$$r_j=-k_{d_j}\cdot C_{S_j}\cdot F_{auto}\cdot\sum_{i=1}^{N}\alpha_{i,j}+\sum_{i=1}^{N}\alpha_{j,i}\cdot F_{auto}\cdot k_{d_i}\cdot C_{S_i} \tag{6}$$

$$F_{auto} = \left(1 - 0.99 \cdot \frac{C_{HC_1}}{C_t}\right)^{\beta_{i,j}} \quad (7)$$

$$F_{auto} = \left(1 - 0.99 \cdot \frac{m_{HC_2}}{m_{HC_{2o}}}\right)^{\beta_{i,j}} \quad (8)$$

Eq. (6) shows the overall kinetic for each solid compound, which is formed by two parts. The first represents the breaking of this compound into any product of lower molecular weight. Meanwhile, the second shows the formation of this compound from any component of higher molecular weight (Fig. 3b). Eqs. (7) and (8) presents two coefficients. The initial velocity factor, whose recommended value is 0.99 (Capart et al., 2004), and the acceleration factor ($\beta_{i,j}$), which represents how fast the degradation is once the fractionation process has started. In the same way, the deacetylation kinetics were also defined by an autocatalytic expression for each compound of both hemicellulose populations (Eqs. (9) and (10)) respectively.

$$r_{dea_j} = k_{d_j} \cdot C_{s_j} \cdot \left(1 - 0.99 \cdot \frac{C_{s_j}}{C_t}\right)^{\beta_{i,j}} \cdot \left(1 - 0.99 \cdot \frac{C_{s_{HC_1}}}{C_t}\right)^{\gamma_{i,j}} \quad (9)$$

$$r_{deai_j} = k_{d_j} \cdot C_{s_j} \cdot \left(1 - 0.99 \cdot \frac{m_{HC_1}}{m_{HC_{1o}}}\right)^{\gamma_{i,j}} \quad (10)$$

Finally, the direct deacetylation reactions from hemicellulose are shown in Eqs. (11)–(13) the oligomer and monomer production (C5) in Eq. (14) and the dimer and monomer formation (C6) in Eq. (15).

$$r_{dead} = k_{dead} \cdot C_{s_{HC_1}} \cdot \left(1 - 0.99 \cdot \frac{C_{s_{HC_1}}}{C_t}\right)^{\beta_{i,j}} \quad (11)$$

$$r_{deadi} = k_{deadi} \cdot C_{s_{HC_2}} \cdot \left(1 - 0.99 \cdot \frac{C_{s_{HC_1}}}{C_t}\right)^{\beta_{i,j}} \quad (12)$$

$$r_{deadii} = k_{deadii} \cdot C_{s_{HC_2}} \quad (13)$$

$$r_{cv} = k_{cv} \cdot C_{s_{HC_1}} \quad (14)$$

$$r_{lent} = k_{lent} \cdot C_{s_{HC_1}} \cdot \left(1 - 0.99 \cdot \frac{C_{s_{HC_1}}}{C_t}\right)^{\beta_{i,j}} \quad (15)$$

3.3.2.1. Liquid phase. Liquid phase kinetics were defined in a similar way to solid phase kinetics but including the effect of the proton concentration, which works as a catalytic reaction (Eq. (16)).

$$r_j = -k_{L_j} \cdot C_{L_j} \cdot C_{H^+}^{n_1} \cdot \sum_{i=1}^{N} \alpha_{i,j} + \sum_{i=1}^{N} \alpha_{j,i} \cdot C_{H^+}^{n_1} \cdot k_{L_i} \cdot C_{L_i} \quad (16)$$

Moreover, in liquid phase there are sugar degradation, sugar deacetylation and repolymerization from degradation products reactions whose kinetics are shown by Eqs. (17)–(19) respectively. In Eq. (17) the addition of the sugar concentration was needed because they were calculated separately depending on their origin: C_1, C_2, HC_1, HC_2 or deacetylated fibers (from HC_1 and HC_2). In addition, the dissolution acetic acid equilibrium and the proton consumption reactions are arrayed in Eqs. (20) and (21) respectively.

$$r_{deg} = \left(k_{deg1} \cdot \sum_{i=1}^{i=2} C_{L_{i_{Sugar-C6}}}^{n_2} + k_{deg2} \cdot \sum_{i=1}^{i=4} C_{L_{i_{Sugar-C5}}}^{n_d}\right) \cdot C_{H^+}^{n_2} \cdot \left(1 - 0.99 \cdot \frac{C_{s_{HC_1}}}{C_t}\right)^{\beta_{ij}} \quad (17)$$

$$r_{de} = k_{de} \cdot C_{L_{Sugar}} \quad (18)$$

$$r_{rep} = k_{rep} \cdot C_{L_{DP}} \quad (19)$$

$$r_{acet} = k_{direct} \cdot C_{L_{acet}} - k_{inverse} \cdot C_{L_{acet^-}} \cdot C_{H^+} \quad (20)$$

$$r_{prot} = k_{prot} \cdot C_{L_{base}} \quad (21)$$

3.3.2.1. Kinetic constants. Kinetic constants for biomass fractionation were defined to include the effect of the polymerization degree (molecular weight) of the reactive and the changes in biomass structure and water properties during the process. Therefore, all of them were defined by the expression (22). Where R is the ideal gas constant ($8.314\,J \cdot mol^{-1} \cdot K^{-1}$) and T the operating temperature (°C).

$$k_{d_j} = k_{L_j} = e^{A(T) - \frac{(E_1 + E_2 \cdot PD_j)}{R \cdot T}} \quad (22)$$

The other kinetic constants were defined by the following expressions.

$$k_{dead} = e^{A - \frac{(E_1)}{R \cdot T}} \quad (23)$$

$$k_{deadi} = e^{A - \frac{(E_1 + E_2 \cdot PD_{HC})}{R \cdot T}} \quad (24)$$

$$k_{deadii} = e^{A - \frac{(E_1)}{R \cdot T}} \quad (25)$$

$$k_{cv} = e^{A - \frac{(E_1 + E_2 \cdot PD_{HC})}{R \cdot T}} \quad (26)$$

$$k_{lent} = e^{A - \frac{(E_1 + E_2 \cdot PD_{HC})}{R \cdot T}} \quad (27)$$

$$k_{deg} = e^{A - \frac{(E_1 + E_2 \cdot 1)}{R \cdot T}} \quad (28)$$

$$k_{de} = e^{A - \frac{(E_1 + E_2 \cdot 1)}{R \cdot T}} \quad (29)$$

$$k_{rep} = e^{A(T) - \frac{(E_1)}{R \cdot T}} \quad (30)$$

$$k_{direct} = e^{A - \frac{(E_1)}{R \cdot T}} \quad (31)$$

$$k_{inverse} = e^{A - \frac{(E_1)}{R \cdot T}} \quad (32)$$

$$k_{prot} = e^{A - \frac{(E_1)}{R \cdot T}} \quad (33)$$

3.3.2.2. Proton reaction order. Proton concentration was considered in Eqs. (16) and (17) because it is the main cause of biomass hydrolysis and it has a high effect in sugar degradation (Li et al., 2014). In order to obtain a theoretical value of its reaction order, the following process was done. As protons have a catalytic role, their effect in a general kinetic would be described by Eq. (34).

$$K = e^{A - \frac{(E_1 + f(C_{H^+}))}{R \cdot T}} = e^{A} \cdot e^{-\frac{(E_1)}{R \cdot T}} \cdot e^{-\frac{f(C_{H^+})}{RT}} \quad (34)$$

If the function of the proton concentration would be logarithmic, e.g. ($f(C_{H^+}) = \ln(C_{H^+})$), Eq. (34) could be rewritten into Eq. (35).

$$K = e^{A - \frac{(E_1 + f(C_{H^+}))}{R \cdot T}} = e^{A} \cdot e^{-\frac{(E_1)}{R \cdot T}} \cdot C_{H^+}^{-\frac{1}{R \cdot T}} \quad (35)$$

Therefore, the reaction order of the protons would depend directly proportional on temperature.

3.3.2.3. Stoichiometric matrix. All the equations were used in mass basis so their stoichiometric coefficients ($\alpha_{i,j}$) were in mass basis too. They were defined in order to represent the cleavage of a polysaccharide fiber into any smaller compound (Fig. 3b). In addition, it was considered that any fiber mainly breaks into

near oligomers (Eq. (36)). This was supposed because during fractionation, biomass is slowly solved up to certain time is reached, when, suddenly its extraction rate is largely increased. On the other hand, for the deacetylation, it was assumed that if the PD is greater than 19 an average deacetylated oligomer is produced and, if it is lower, one of the other 19 deacetylated oligomers is released. The breaking of these 20 deacetylated compounds was simulated as if their highest oligomer would have a PD of 20. This is done to include the fiber degradation during the deacetylation. Furthermore, the last assumption is supposed because the deacetylation would take place when biomass have been degraded into relative low PD oligomer.

$$\alpha_{i,j} = \frac{\frac{\left(\frac{PD_j}{PD_i}\right)}{PD_j - PD_i}}{\sum_{i=1}^{N} \frac{\left(\frac{PD_j}{PD_i}\right)}{PD_j - PD_i}}; \quad \alpha_{1,j} = 0 \tag{36}$$

For deacetylation it was considered that 1.0 g of reactive produces 0.3 g of acetic acid and 0.7 g of deacetylated oligomer. For the acetic acid equilibrium it was supposed that 1 g of acetic acid generates 0.017 g protons and 0.983 g of residue. For hexoses deacetylation, it was assumed that 0.33 g of acetic acid and 0.67 g of degradation products are produced. For direct formation of monomer from hemicellulose (C5), 1 g of hemicellulose generates 0.15 g of monomer and 0.85 g of oligomer of 191 units. And for direct formation of monomer from cellulose (C6), 1 g of cellulose generates 0.5 g of monomer and 0.5 g of dimer (cellobiose). The values of the coefficients above mentioned were obtained during the optimization. For proton consumption, it was assumed that 0.2 g react with 0.8 g of base material.

3.3.3. Solubility

Eqs. (1), (3) and (5) show an equilibrium concentration in liquid phase (C_{Lj}^*) which is obtained by the product of an equilibrium constant (H_j) and the concentration in the solid ($C_{Lj}^* = H_j \cdot C_{sj}$). This equilibrium constant represents the solubility of biomass and it should be a function of several variables: the polymerization degree, structure of the biopolymer, acetylation degree and some water properties (Kruse and Dinjus, 2007; Miller-Chou and Koenig, 2003; Teo et al., 2010). In order to include these aspects in its calculation, Eq. (37) was used.

$$H_j = \frac{H_o(T) \cdot T}{1 + e^{h_p \cdot (PD - PD_h)}} \tag{37}$$

3.4. Resolution

The combination of Eqs. (3) and (5) generates a set of partial differential equations (PDE) which need to be discretized to convert them into a set of ordinary differential equations (ODE). The discretization was performed by the combination of the orthogonal colocation method on finite elements (Press et al., 2007). Once the discretization has been done, the set of ODE was solved by the Runge–Kutta's method with an 8th convergence order. The fitting of the experimental data implied an optimization problem. Due to its complexity, it was previously initialized by solving it by hand, and then, optimized by the Nelder–Mead–Simplex's method. Finally, the solution was reviewed in order to ensure the physical meaning of the parameters. The objective function was the minimization of the Absolute Average Deviation (A.A.D., Eq. (38)) for TOC, acetic acid, sugar and degradation products concentration at the reactor output (given a higher weight to the TOC values).

$$\text{A.A.D.} = \sum_{i=1}^{n} \frac{1}{n} \cdot \left| \frac{X_{exp} - X_{sim}}{X_{exp}} \right| \cdot 100 \tag{38}$$

4. Results and discussion

4.1. Effect of volumetric flow and temperature

In this part, the role of the volumetric flow and the operating temperature is assessed. The former is shown in Fig. 4a by the TOC evolution at 3 different volumetric flows (11.5, 15.0, and 27.0 mL/min) and at the same temperature range (180–260 °C). Apart from dilution, the following effects can be observed. At 180 °C the volumetric flow does not change the time of the maximum TOC value but it enhances the extraction, reducing the time of the final part of this stage. After the temperature change, flow again accelerates the process but it also modifies highly the maximum TOC time. This behavior could be explained by the fact that at 180 °C biomass degrading would be slow enough to break into oligomers and not directly to dimers or monomers (with greater water solubility). So, an increment in the water velocity only affect to the end of this stage, when more soluble components would be produced. In contrast, at 260 °C biomass would be highly degraded, producing and enormous amount of soluble compounds and the volumetric flow would affect from the beginning. In addition, in this second stage a slow variation zone at the end of the process is observed because, at this time, biomass would be formed by very low soluble substances, such as deacetylated oligomers. Therefore, during the operation, 3 zones can be observed depending on the controlling resistance of the mass transfer. Two zones controlled by the solubility (for the first 10 min and at the end of the process) and other zone dominated by the external mass transfer (from 10 min and until the temperature change). Being this latter, the zone where a change in volumetric flow can influence on the extraction. On the contrary, temperature affects to the whole process (Fig. 4b) which could be explained by the bigger formation of soluble compounds at higher temperatures.

On the other hand, the final mass of the solid presented an interesting result (Table 2). It can be checked that the recovered mass after the operation (m_{Real}) was always lower than the lignin content of the sample (m_{Lignin}), which at this conditions should behave as an inert. This discrepancy could be explained by a weakening of biomass structure due to the operation at two temperatures. So, after the second temperature change, some parts of biomass could be broken and fluidized. Finally, it can also be observed that temperature has an inverse proportional ratio to the final mass of the solid, which boosts the idea of a thermal breaking process.

4.2. Fittings

The validation of the model was performed by fitting the TOC for the experiments arrayed in Table 1. In addition, acetic acid concentration, sugars C5 and C6 concentration and degradation products concentration were simulated and checked with their experimental values for essays 2–5. For the latter, these fittings and simulations are showed in Fig. 5. The obtained parameters for all of them are listed in Table 4.

Analyzing Fig. 5a it can be observed that the extraction was slow up to 10 min when the TOC suddenly increases. This also occurs in the acetic acid (Fig. 5b), C5 and C6 sugar concentration (Fig. 5c and d respectively) and degradation products concentration (Fig. 5e). This behavior could by caused by two reasons. The first could be that, up to this time, biomass degradation was not big enough to produce high soluble compounds (as it was mentioned in Section 4.1). The second could be that, in parallel to oligomer formation, an acetic acid production (and releasing) takes places, enhancing the hydrolysis. After the maximum TOC value (14 min), a slower extraction was observed in all the profiles

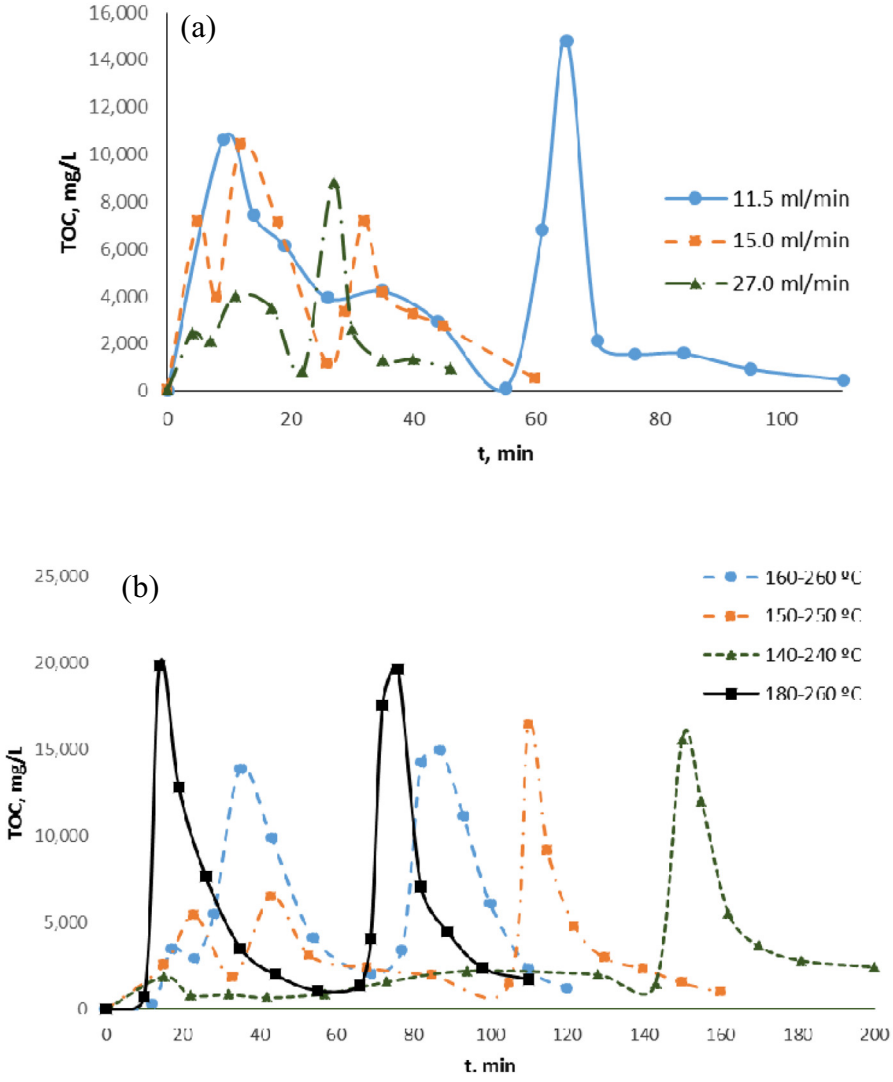

Fig. 4. TOC evolution with volumetric flow (a) and temperature (b).

Table 2
Final solid mass evolution.

Experiment	m_{Real} [1] g	m_{Lignin} [2] g
1	0.2622	1.7227
2	0.4659	1.7311
3	0.8491	1.7508
4	0.8733	1.7288
5	0.4380	1.7525
6	0.4601	1.7423
7	0.8491	1.7616
8	0.8491	1.7394

[1] Measured final solid mass.
[2] Lignin content of the sample and final mass expected after the operation.

of Fig. 5, which was attributed to a mass transfer limitation. In addition, biomass would be more and more composed by low soluble products, such as deacetylated oligomers, HC_2 and C_2. This behavior continued up to the temperature change was performed (55 min), obtaining a similar behavior to the first step. Nevertheless, an initial slow period is not present due to the fact that at 260 °C biomass degradation is so high that soluble compounds are directly produced. From this adjustment it can be concluded that the model is suitable to simulate a biomass fractionation process. The same conclusion can be obtained from the value of the A.A.D. for each assay (Table 3). Which were relatively low taking into account the complexity of the reaction process, the little amount of initial raw material, the diversity of biomass and the dilution of the outlet stream. This latter would increase the average deviation from 33% at low flow (experiments 1–5) up to 58% at high flow (experiments 6–8). Focusing in the calculated values, it can be seen that the lowest deviations were in TOC fittings (42.62%). The experimental data of sugar and degradation product of experiment 1 were not considered because their values showed discrepancy with the tendency fixed by experiments 2–5. In the case of experiments 6 and 7, only TOC was considered due to the high dilution of these samples.

4.2.1. Fitted parameters

In this section an analysis of the parameters showed in Table 4 is done. It is interesting the fact that the obtained kinetic parameters (A, $\beta_{i,j}$ and $\gamma_{i,j}$) show changes around 150 and 240 °C. Temperatures that represent the star of the fast degradation of hemicellulose and cellulose respectively (Kumar et al., 2010; Minowa et al., 1998; Pronyk and Mazza, 2010; Rissanen et al., 2014). Therefore, the tendency calculated for these variables agrees with the data reported by other authors, showing that the model is

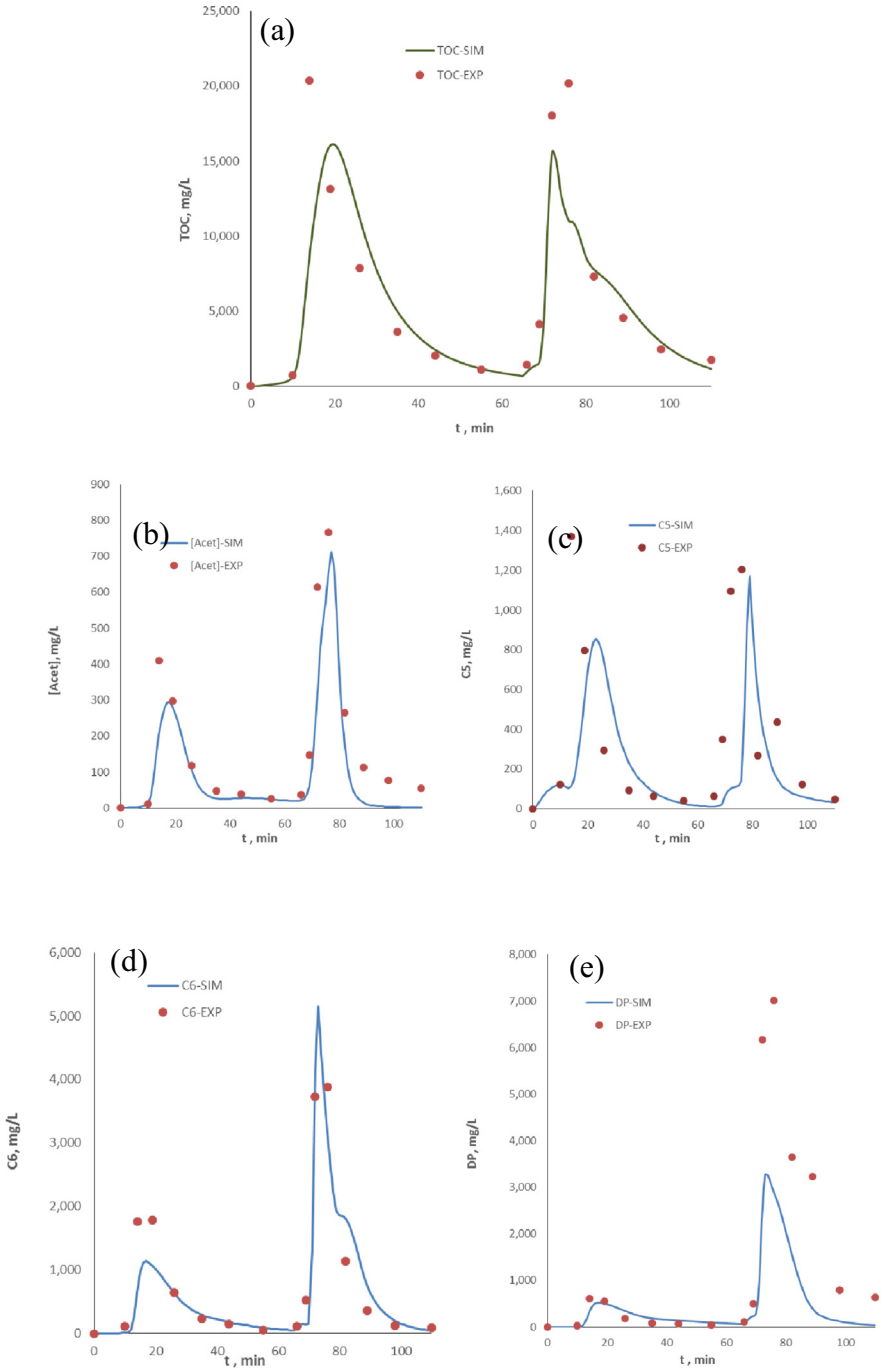

Fig. 5. Adjustment of the experiment 5. TOC fitting (a), simulation of the concentration of acetic acid (b), sugars C5 (c), sugars C6 (d) and degradation products (e).TOC-EXP: measured TOC. TOC-SIM: simulated TOC. [Acet]-EXP: measured acetic acid concentration. [Acet]-SIM: simulated acetic acid concentration. C5-EXP: measured C5 sugar concentration. C5-SIM: simulated C5 sugar concentration. C6-EXP: measured C6 sugar concentration. C6-SIM: simulated C6 sugar concentration. DP-EXP: measured degradation products concentration. DP-SIM: simulated degradation products concentration.

able to reproduce the process with physical meaning. Regarding the equilibrium constants (H_j), it is observed that for C_1 and C_2 the opposite behavior is obtained. The first increases its value with temperature up to 240 °C and the second is constant until 180 °C, where in starts to grow. This behavior could be explained by the fact that C_1 should be more soluble than C_2 due to its lack of crystallinity. So, the former would increase its water solubility up to it would be totally soluble. The later, by the contrary, would have a low (and constant) solubility up to certain temperature when it would start to solve more and more due to the change in water properties. Hemicelluloses show the same tendency that C_1 but with smoother changes because of they are more soluble. It is also interesting that the polymerization constant decreases at 240 °C, which would be originated because of the bonds breaking would be bigger than the repolymerization at high temperatures. Finally, it is remarkable that the reaction order for proton increases with temperature, confirming the theoretical development showed in Section 3.3.2.2.

4.2.1.1. Acceleration factors. Effect of temperature and volumetric flow. Temperature and flow influence on the acceleration factors in an opposite way, increasing and decreasing them respectively.

Table 3
A.A.D. of the fittings.

Experiment	A.A.D.				
	TOC	[Acetic acid][1]	C5[2]	C6[3]	DP[4]
1	51.15	61.06	*	*	*
2	24.55	49.51	54.75	65.45	48.56
3	34.61	56.26	60.58	60.79	77.02
4	25.36	47.11	51.78	57.87	66.24
5	30.15	45.02	73.56	49.56	75.35
6	63.36	*	*	*	*
7	53.29	*	*	*	*
8	58.47	*	*	*	*
Average	42.62	51.79	60.17	58.42	66.79

[1] Acetic acid concentration.
[2] Sugars C5 concentration.
[3] Sugars C6 concentration.
[4] Degradation products concentration.
* Experimental data which were not considered.

Regarding temperature, the behavior could be explained because of a higher temperature means more biomass degradation, more oligomer production and, due to this, a more abrupt process. In contrast, a greater flow would reduce the residence time of the products, enhancing the extraction (if temperature is high enough). So, oligomer would have less time to degrade and the fractionation would be smoother.

4.2.1.2. Hemicellulose and cellulose composition. In the Section 3.2 it was assumed that two types of hemicelluloses (HC_1 and HC_2) and cellulose (C_1 and C_2) can be present in biomass. Therefore, their initial composition constituted other 2 parameters to fit. The calculated value for HC_1 and C_1 were 75% and 30% of the total hemicellulose and cellulose content, respectively. This result agrees with the expected behavior because, in general, cellulose is more difficult to extract than hemicellulose. So, C_2 and HC_1 would be the main components in biomass. In addition, these val-

Table 4
Fitted parameters for solid (4.1) and liquid phase (4.2).

Solid phase

HC_1 population

r_j

$$k_d = e^{A-\frac{7550-0.1*PD}{T+273.15}}$$
$$A = 16.16 + \frac{0.24}{1+e^{-(T-145)}} + \frac{1.10}{1+e^{-(T-245)}}$$
$$\beta_{i,j} = 20 + \frac{2}{1+e^{-(T-160)}}$$

H_j

$$H_j = \frac{h_o \cdot T}{1+e^{0.08\cdot(PD-3)}}$$

No deacetylated

$$h_o = \frac{0.003}{1+e^{(T-160)}} + \frac{-5\cdot10^{-7}\cdot T^2+2.64\cdot10^{-4}-0.019182}{1+e^{-(T-156)}}$$

Deacetylated

$$h_o = 0.005$$

r_{dea_j}

$$k_d = e^{12.0-\frac{7550-0.1*PD}{T+273.15}}$$
$$\beta_{i,j} = 200 - \frac{80}{1+e^{-(T-155)}}$$
$$\gamma_{i,j} = \frac{15}{1+e^{-(T-155)}}$$

r_{dead}

$$k_{dead} = e^{12.0-\frac{7550-0.1*200}{T+273.15}}$$
$$\beta_{i,j} = 50 + \frac{10}{1+e^{-(T-155)}}$$

r_{cv}

$$k_{cv} = e^{11.2-\frac{7550-0.1*200}{T+273.15}}$$

r_{lent}

$$k_{lent} = e^{12.0-\frac{8000-0.1*200}{T+273.15}}$$
$$\beta_{i,j} = 7 + \frac{1}{1+e^{-(T-155)}}$$

C_1 population

r_j

$$k_d = e^{A-\frac{8000-0.1*PD}{T+273.15}}$$
$$A = 18.5$$
$$\beta_{i,j} = \frac{15}{1+e^{-(T-160)}}$$

H_j

$$H_j = \frac{h_o \cdot T}{1+e^{0.08\cdot(PD-1)}}$$
$$h_o = \frac{0.0011\cdot T-0.0144}{1+e^{(T-250)}} + \frac{0.012}{1+e^{-(T-250.2)}}$$

HC_2 population

r_j

$$k_d = e^{A} - \frac{7550-0.1*PD}{T+273.15}$$
$$A = 12 + \frac{4}{1+e^{-(T-245)}}$$
$$\beta_{i,j} = \frac{1}{1+e^{-(T-165)}} + \frac{30}{1+e^{-(T-245)}}$$

H_j

$$H_j = \frac{h_o \cdot T}{1+e^{0.08\cdot(PD-3)}}$$

No deacetylated

$$h_o = \frac{0.003}{1+e^{(T-160)}} + \frac{-5\cdot10^{-7}\cdot T^2+2.64\cdot10^{-4}-0.019182}{1+e^{-(T-156)}}$$

Deacetylated

$$h_o = 0.005$$

r_{dea_j}

$$k_d = e^{12.5-\frac{7550-0.1*PD}{T+273.15}}$$
$$\gamma_{i,j} = 5$$

r_{deadi}

$$k_{deadi} = e^{7.5-\frac{6392}{T+273.15}}$$
$$\beta_{i,j} = 15 + \frac{55}{1+e^{-(T-155)}}$$

r_{deadii}

$$k_{deadii} = e^{1-\frac{6392}{T+273.15}}$$

C_2 population

r_j

$$k_d = e^{A-\frac{8000-0.1*PD}{T+273.15}}$$
$$A = 17.50 + \frac{0.5}{1+e^{-(T-245)}}$$
$$\beta_{i,j} = 4$$

H_j

$$H_j = \frac{h_o \cdot T}{1+e^{0.08\cdot(PD-1)}}$$
$$h_o = \frac{0.001}{1+e^{(T-180)}} + \frac{9\cdot10^{-5}-0.0152}{1+e^{-(T-180)}}$$

Liquid phase

r_j

k_{d_j} = *Kinetic constants in solid phase*

$$n_1 = 0.361\cdot\ln(T) - 1.6165$$

r_{deg}

$$k_{deg1} = e^{10.0-\frac{7550-0.1*1}{T+273.15}}$$
$$k_{deg2} = e^{17.0-\frac{8000-0.1*1}{T+273.15}}$$
$$n_d = 0.6$$
$$n_2 = 0.361\cdot\ln(T) - 1.7785$$
$$\beta_{i,j} = \frac{2.50\cdot T}{1+e^{(T-165)}} + \frac{50}{1+e^{-(T-165)}}$$

r_{de}

$$k_{de} = e^{11.0-\frac{7550-0.1*1}{T+273.15}}$$

r_{rep}

$$k_{rep} = 17.3 - \frac{1.3}{1+e^{-(T-255)}}$$

r_{acet}

$$k_{direct} = e^{0.5-\frac{1053}{T+273.15}}$$
$$k_{inverse} = e^{1.76-\frac{1053}{T+273.15}}$$

r_{prot}

$$k_{prot} = e^{3.36-\frac{1170}{T+273.15}}$$

HC_1 population

r_j

$$\beta_{i,j} = 0$$

C_1 population

r_j

$$\beta_{i,j} = 0$$

HC_2 population

r_j

$$\beta_{i,j} = \frac{22{,}793\cdot Q^{-3033}}{1+e^{-(T-165)}}$$

C_2 population

r_j

$$\beta_{i,j} = 4 - \frac{3}{1+e^{-(Q-14)}}$$

Other parameters

Mass transfer coefficient

$$k_j \cdot a = 0.2\cdot u^{0.2}\cdot(1-\varepsilon)$$

H_{acet}

$$H_{acet} = 0.025\cdot T$$

H_{rep}

$$H_{rep} = 0.008\cdot T$$

ues also agree with literature (Charles et al., 2004; Klemm et al., 2005; Parajó et al., 2004). For HC_1 has been reported that its value is between 65% and 90% of the total hemicellulose and for C_2 around 65%.

4.3. Simulated behavior

Finally, an overall simulation of the fractionation was performed (Fig. 6 and Table 5). Fig. 6a shows the evolution of the solid composition during the process, which agrees with the experimental data showed in 4.2.1. During the first stage, hemicellulose is mainly extracted and only a few part of cellulose (C_1) is also recovered. The main part of cellulose (C_2) and a few amount of hemicellulose (HC_2) remain in solid up to the temperature change is done, being solubilized. Finally, the solid is formed by residual cellulose (as cellobiose), deacetylated oligomers and the repolymerization products. Solid phase composition is also represented in Fig. 6c and d by population C_2 and HC_1 evolution respectively. It is remarkable the result for HC_1 because up to 22 min of operation the main products are oligomers. So, this simulation agrees with the explanation given in Section 4.1 about the temperature and water flow effect. In addition, these simulations are interesting because they reproduce a real composition of biomass, which could be a mandatory factor to decide when stop the process. On the other hand, liquid behavior is shown in Fig. 6b. At the beginning of the process (until 10 min), mainly sugars would be recovered because biomass has not been fractionated yet. Once this time have been reached, biomass would produce soluble oligomers

Table 5
Simulation of the extracted biomass.

Experiment	m_{Real} [1] g	$m_{Simulated}$ [2] g	$m_{Theoretical}$ [3] g
1	4.2720	3.5948	4.3002
2	4.1968	3.6212	4.3211
3	4.1796	3.8357	4.3704
4	3.5992	3.9716	4.3154
5	3.8850	3.6408	4.3745
6	4.6349	4.0318	4.3491
7	3.7172	4.0280	4.3973
8	3.4134	4.0061	4.3419

[1] Extracted biomass during the process.
[2] Simulated value of the extracted biomass.
[3] Total amount of cellulose and hemicellulose in the solid.

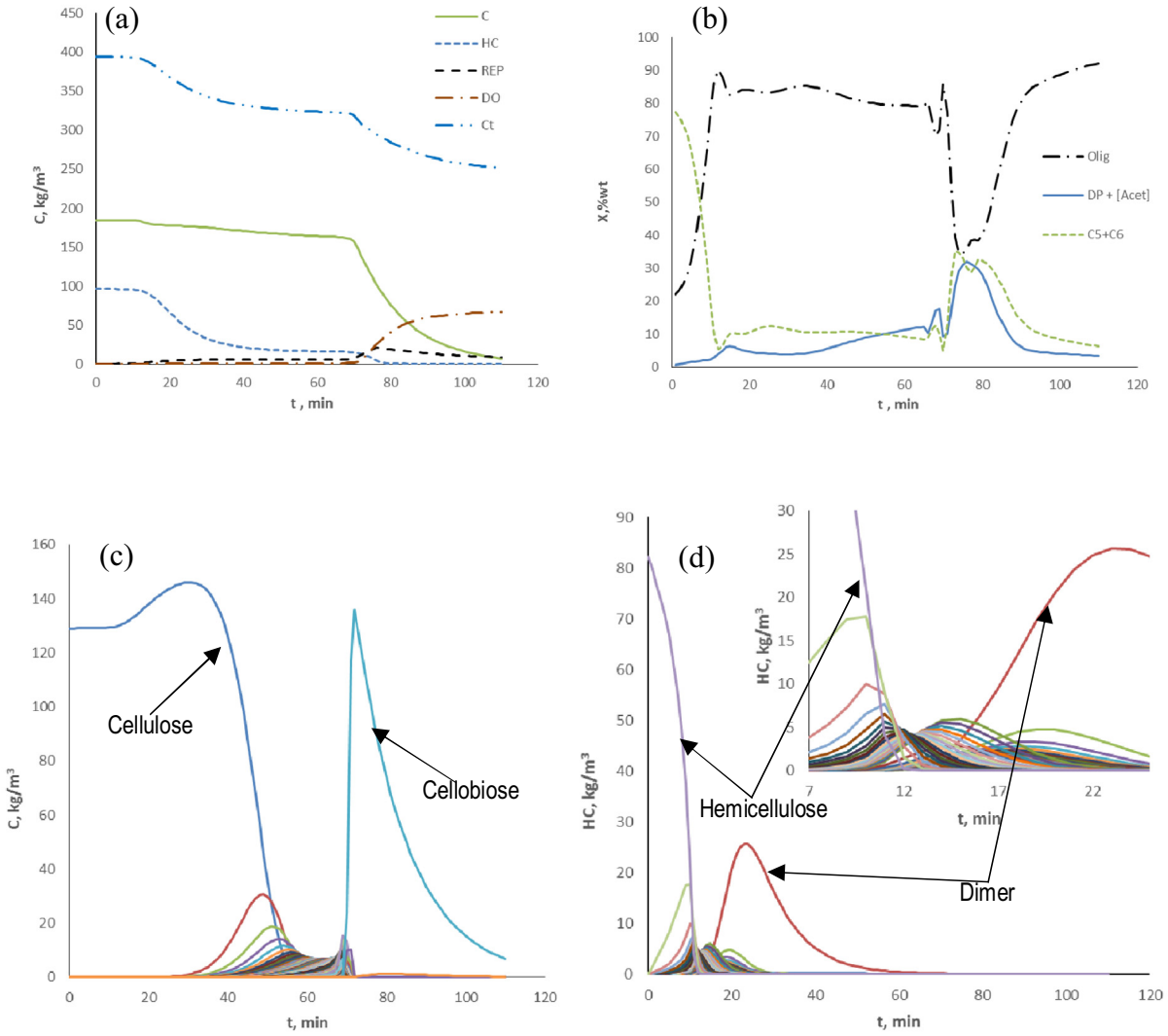

Fig. 6. Overall simulation of the process. (a) Evolution of solid cellulose and hemicellulose. (b) Liquid oligomer concentration. (c) Solid C_2 population evolution. (d) Solid HC_1 population evolution. HC: total solid hemicellulose content. C: total solid cellulose content. REP: polymerization product in the solid. DO: deacetylated product in the solid. Ct: total solid concentration. Olig: liquid oligomer content. DP + [Acet]: addition of the amount of degradation product and acetic acid in the liquid. C5 + C6: total sugar amount in the liquid.

and they would be the main component in the liquid phase. This tendency continuous up to around 60 min, when biomass would be exhausted, and the concentration of oligomers starts to decrease. Moreover, at this time, the temperature change is performed and many degradation products and sugar are produced, increasing their concentrations quickly. At the end of the process, the oligomers would be again the main component in the liquid because only cellobiose, deacetylated oligomers and repolymerization products would remain in the solid.

Finally, the amount of extracted biomass was calculated and compared with the experimental data (Table 5). It can be seen that, generally, the experimental value is bigger than the simulated due to the fluidization process explained in 3.1. Thus, this discrepancy could be another reason for the deviation between the simulated and experimental behavior. It is also remarkable that for experiments 7 and 8 the data are lower than the simulated. Which could be caused by the dilution of the sample in these experiments.

4.4. Model limitations and other biomass

From the discussions showed in Sections 4.2 and 4.3, it can be concluded that the model is able to reproduce the holm oak fractionation in a packed bed reactor at subcritical conditions. However, in order to apply this model to other biomass samples the following statements should be considered:

- The reaction pathway was developed for woody biomass, as hardwood as softwood. Thus, to adjust any other woody species only changes in the parameters or/and in the initial biopolymer length would be required. For other hardwood woods, the changes in the parameters would be required because the fractionation also depends on the structure and chemical properties of biomass.
- Extractives and soluble lignin were assumed as negligible substances. Therefore, to reproduce the behavior of any biomass with a great amount of any of them, such as grape seeds, new mass balances for these compounds should be added.
- The reaction pathway was done assuming that the biomass sample would be composed of cellulose, hemicellulose and lignin. However, there are several species that present other polysaccharides, like starch, which could not be studied with the presented model.
- Lignin as an inert. Lignin does not start its degradation up to 300 °C, however it protects cellulose and hemicellulose against degradation. Therefore, changes in lignin composition would require a new set of parameters to reproduce the biomass breaking.

5. Conclusions

A kinetic model for hydrothermal fractionation of holm oak was developed and validated in this work. This model could reproduce the experimental data considering all the physical phenomena observed, like porosity variations, and the molecular weight distributions. Moreover, a novel reaction pathway based on 4 different populations of oligomers was introduced. These populations were defined according to their origin: hard cellulose, hard hemicellulose, weak cellulose or weak hemicellulose. Finally, the temperature and flow effect was assessed, founding that temperature is the main influencing parameter. The water flow affected to the process only if temperature was high enough to degrade biomass.

Acknowledgements

The authors acknowledge the Spanish Economy and Competitiveness Ministry, Project Reference: ENE2012-33613 for funding. Álvaro Cabeza would like to thank to the Spanish Ministry of Education Culture and Sports, training program of university professors (reference FPU2013/01516) for the research training contract.

References

Alvarez-Vasco, C., Zhang, X., 2013. Alkaline hydrogen peroxide pretreatment of softwood: hemicellulose degradation pathways. Bioresour. Technol. 150, 321–327.
Bobleter, O., 1994. Hydrothermal degradation of polymers derived from plants. Prog. Polym. Sci. (Oxford) 19, 797–841.
Cabeza, A., Sobrón, F., Yedro, F.M., García-Serna, J., 2015. Two-phase modelling and simulation of the hydrothermal fractionation of holm oak in a packed bed reactor with hot pressurized water. Chem. Eng. Sci. 138, 59–70.
Capart, R., Khezami, L., Burnham, A.K., 2004. Assessment of various kinetic models for the pyrolysis of a microgranular cellulose. Thermochim. Acta 417, 79–89.
Carrier, M., Loppinet-Serani, A., Denux, D., Lasnier, J.-M., Ham-Pichavant, F., Cansell, F., Aymonier, C., 2011. Thermogravimetric analysis as a new method to determine the lignocellulosic composition of biomass. Biomass Bioenergy 35, 298–307.
Charles, E.W., Stephen, R.D., Michael, E.H., John, W.B., Catherine, E.S., Liisa, V., 2004. Hydrolysis of cellulose and hemicellulose. In: Polysaccharides. CRC Press.
Feng, Y., Qi, X., Jian, H.L., Sun, R.C., Jiang, J.X., 2012. Effect of inhibitors on enzymatic hydrolysis and simultaneous saccharification fermentation for lactic acid production from steam explosion pretreated lespedeza stalks. BioResources 7, 3755–3766.
Garrote, G., Domínguez, H., Parajó, J.C., 2002. Interpretation of deacetylation and hemicellulose hydrolysis during hydrothermal treatments on the basis of the severity factor. Process Biochem. 37, 1067–1073.
Haghighat Khajavi, S., Kimura, Y., Oomori, T., Matsuno, R., Adachi, S., 2005. Kinetics on sucrose decomposition in subcritical water. LWT Food Sci. Technol. 38, 297–302.
Harmsen, P., Huijgen, W., Bermudez, L., Bakker, R., 2010. Literature review of physical and chemical pretreatment processes for lignocellulosic biomass. Wageningen UR Food & Biobased Res.
Klemm, D., Schmauder, H.-P., Heinze, T., 2005. Cellulose. In: Biopolymers Online. Wiley-VCH Verlag GmbH & Co. KGaA.
Kruse, A., Dinjus, E., 2007. Hot compressed water as reaction medium and reactant: properties and synthesis reactions. J. Supercrit. Fluids 39, 362–380.
Kumar, S., Gupta, R., Lee, Y.Y., Gupta, R.B., 2010. Cellulose pretreatment in subcritical water: effect of temperature on molecular structure and enzymatic reactivity. Bioresour. Technol. 101, 1337–1347.
Li, H.-Q., Jiang, W., Jia, J.-X., Xu, J., 2014. PH pre-corrected liquid hot water pretreatment on corn stover with high hemicellulose recovery and low inhibitors formation. Bioresour. Technol. 153, 292–299.
Lin, R., Cheng, J., Ding, L., Song, W., Qi, F., Zhou, J., Cen, K., 2015. Subcritical water hydrolysis of rice straw for reducing sugar production with focus on degradation by-products and kinetic analysis. Bioresour. Technol. 186, 8–14.
Miller-Chou, B.A., Koenig, J.L., 2003. A review of polymer dissolution. Prog. Polym. Sci. 28, 1223–1270.
Minowa, T., Zhen, F., Ogi, T., 1998. Cellulose decomposition in hot-compressed water with alkali or nickel catalyst. J. Supercrit. Fluids 13, 253–259.
Mohan, M., Banerjee, T., Goud, V.V., 2015. Hydrolysis of bamboo biomass by subcritical water treatment. Bioresour. Technol. 191, 244–252.
Parajó, J.C., Garrote, G., Cruz, J.M., Dominguez, H., 2004. Production of xylooligosaccharides by autohydrolysis of lignocellulosic materials. Trends Food Sci. Technol. 15, 115–120.
Press, W., Teukolsky, S., Vetterling, W., Flannery, B., 2007. Numerical Recipes: The Art of Scientific Computing, third ed. Cambridge University Press, New York.
Pronyk, C., Mazza, G., 2010. Kinetic modeling of hemicellulose hydrolysis from triticale straw in a pressurized low polarity water flow-through reactor. Ind. Eng. Chem. Res. 49, 6367–6375.
Ranzi, E., Cuoci, A., Faravelli, T., Frassoldati, A., Migliavacca, G., Pierucci, S., Sommariva, S., 2008. Chemical kinetics of biomass pyrolysis. Energy Fuels 22, 4292–4300.
Rissanen, J.V., Grénman, H., Willför, S., Murzin, D.Y., Salmi, T., 2014. Spruce hemicellulose for chemicals using aqueous extraction: kinetics, mass transfer, and modeling. Ind. Eng. Chem. Res. 53, 6341–6350.
Rogalinski, T., Liu, K., Albrecht, T., Brunner, G., 2008. Hydrolysis kinetics of biopolymers in subcritical water. J. Supercrit. Fluids 46, 335–341.
Tanoue, K.I., Hinauchi, T., Oo, T., Nishimura, T., Taniguchi, M., Sasauchi, K.I., 2007. Modeling of heterogeneous chemical reactions caused in pyrolysis of biomass particles. Adv. Powder Technol. 18, 825–840.
Teo, C.C., Tan, S.N., Yong, J.W.H., Hew, C.S., Ong, E.S., 2010. Pressurized hot water extraction (PHWE). J. Chromatogr. A 1217, 2484–2494.
Tock, L., Gassner, M., Maréchal, F., 2010. Thermochemical production of liquid fuels from biomass: thermo-economic modeling, process design and process integration analysis. Biomass Bioenergy 34, 1838–1854.
Yedro, F.M., Cantero, D.A., Pascual, M., García-Serna, J., Cocero, M.J., 2015. Hydrothermal fractionation of woody biomass: lignin effect on sugars recovery. Bioresour. Technol. 191, 124–132.
Zhu, G., Zhu, X., Xiao, Z., Zhou, R., Zhu, Y., Wan, X., 2014. Kinetics of peanut shell pyrolysis and hydrolysis in subcritical water. J. Mater. Cycles Waste Manage. 16, 546–556.